Hydrogenation of Carbon Nanotubes and Graphite in Liquid Ammonia

S. Pekker*

Research Institute for Solid State Physics and Optics, Hungarian Academy of Sciences, H-1525 Budapest, P.O. Box 49, Hungary

J.-P. Salvetat

CNRS, Centre de Recherches sur la Matière Divisée, 1b Rue de la Férollerie, F-45071 Orléans Cedex 2, France

E. Jakab

Chemical Research Center, Hungarian Academy of Sciences, H-1525 Budapest, P.O. Box 17, Hungary

J.-M. Bonard

Institut de Physique Expérimentale, Ecole Polytechnique Fédérale de Lausanne, CH-1015 Lausanne, Switzerland

L. Forró

Institut de Génie Atomique, Ecole Polytechnique Fédérale de Lausanne, CH-1015 Lausanne, Switzerland

Received: February 18, 2001; In Final Form: June 14, 2001

We have prepared hydrogenated single-wall and multiwall carbon nanotubes, as well as graphite, via a dissolved metal reduction method in liquid ammonia. The hydrogenated derivatives are thermally stable up to 400 °C. Above 400 °C, a characteristic decomposition takes place accompanied with the simultaneous formations of hydrogen and a small amount of methane. Transmission electron micrographs show corrugation and disorder of the nanotube walls and the graphite layers due to hydrogenation. The average hydrogen contents determined from the yield of evolved hydrogen correspond to the compositions of $C_{11}H$ for both types of nanotubes and C_5H for graphite. Hydrogenation occurred even on the inner tubes of multiwall nanotubes as shown by the chemical composition and the overall corrugation. The thermal stability and structural results suggest the formation of C−H bonds in nanotubes and graphite.

1. Introduction

In the past few years, the interesting physical properties of carbon nanotubes have attracted great attention among physicists and material scientists. The first experiments after the discovery[1] focused on preparation[2] and purification[3,4] techniques as well as on understanding the structure and physical properties[5] of the pristine nanotubes. Chemical modifications were restricted to a few reactions such as opening the tubes by selective oxidation[6−8] to fill the central hollow with various materials[9,10] and doping the tubes with alkali metals.[11,12] A more systematic study of the chemical reactivity is desirable for further practical application of the nanotubes. Recently, chemical functionalization came into focus[13−16] since it is an obvious way to modify the chemical and physical properties of the surface of the tubes. Functionalized nanotubes can undergo further chemical reactions producing composites with a variety of materials, like for example polymers. The chemical properties of carbon nanotubes lie between those of graphite and fullerenes. Graphite is chemically inert and, besides the ionic intercalated compounds, only fluorinated and oxidized derivatives can be produced without destroying the layer structure.[17] On the other hand, the functionalization of fullerenes is rather easy as illustrated by the thousands of covalent derivatives prepared so far.[18] Although most of the properties of nanotubes resemble those of graphite, the curvature of their graphene sheets may result in an increased chemical reactivity toward the formation of covalent bonds in the outer surface. Since hydrogenation can be considered as a prototype of chemical functionalization, in this paper we describe the preparation, structure and thermal stability of hydrogenated carbon nanotubes. To determine the reactivity of various carbonaceous materials with respect to hydrogenation we performed the same reaction on single-wall nanotubes (SWNT-s), multiwall nanotubes (MWNT-s), extracted fullerene soot and two types of graphite.

2. Experimental Section

Powder of MWNT-s was produced by arc discharge[1] and purified by a nondestructive sedimentation method.[3] Aqueous SWNT suspension (Tubes@Rice) was filtered and dried, and the resulting "bucky paper" was annealed in a vacuum at 950 °C. Graphite powder was prepared by grinding of soft graphite rods (Johnson Mattey, ultra carbon). Besides graphite powder, turbostratic graphite flakes were also studied. The light-gray powder of this sample consisted of disk-shape particles with typical diameter of 100 nm and thickness of 20 nm. Fullerene

* Corresponding author. E-mail: pekker@szfki.hu.

10.1021/jp010642o CCC: $20.00
Published on Web 07/26/2001

soot was produced by arc discharge. The fullerenes were then extracted in toluene and the residue was dried in a vacuum before use.

A dissolved metal reduction method was applied to perform the hydrogenation of the above carbonaceous materials. Typically 200 mg of carbon and 100 mg of Li was mixed in a glovebox, and the reaction tube was then attached to a vacuum line. Dried NH_3 (20 mL) was condensed to the reaction mixture from a Na/NH_3 solution. The suspension was stirred for an hour at about 220 K, and NH_3 was then evaporated by heating the mixture to ambient temperature. After a second condensation of 20 mL of NH_3, 5 mL of methanol was added slowly to the reactants. After the solvent became colorless, the reaction mixture was gradually heated to ambient temperature to evaporate NH_3. The black product was washed subsequently with methanol, water, dilute hydrochloric acid, water, and methanol. Finally the sample was dried in a vacuum at ambient temperature.

The chemical composition and the thermal stability of the samples was studied by thermogravimetry-mass spectrometry (TG-MS). The TG-MS instrument consists of a Perkin-Elmer TGS-2 thermobalance and a HIDEN HAL 2/301 PIC quadrupole mass spectrometer. Approximately 5 mg samples were heated at a 20 °C/min heating rate from 30 °C to 900 °C in argon atmosphere. A portion of the volatile products was introduced into the mass spectrometer operating at 70 eV in electron impact ionization mode. The intensities of 48 selected ions were monitored together with the thermogravimetric parameters. The intensities were normalized to the ^{38}Ar isotope of the carrier gas in order to avoid errors caused by the shift of the MS sensitivity. The calibration of the MS signals was carried out using a hydrogenated graphite sample heat treated at 350 °C, where the total weight loss was due to hydrogen and methane evolution. The relative proportions of hydrogen and methane were calculated from the integrated intensities applying the ionization efficiency factors[19] of 0.3 and 0.5, respectively. The MS detection of the volatile products is necessary for a quantitative analysis because volatile impurities with higher molecular mass can contribute to the mass loss significantly. Thus, TG method itself overestimates the hydrogen content, as shown recently.[20]

High-resolution transmission electron microscopy was performed by a Philips CM300 electron microscope operating at 300 kV electron energy with a resolution of 0.19 nm.

The electronic properties of hydrogenated MWNT-s were tested by electron spin resonance (ESR) and d.c. transport measurements. The ESR experiment was performed on 2 mg powder of hydrogenated MWNT-s, while for resistivity measurement a thin film was prepared as described previously.[21]

3. Results

3.1. The Hydrogenation Reaction. Hydrogenation of the carbonaceous materials was performed via a dissolved metal reduction method with Li and methanol in liquid ammonia, which can be considered as a modified Birch reduction method. Birch reduction can be applied for the partial reduction of conjugated systems and a similar reaction was used previously for the hydrogenation of fullerenes.[22] Besides Birch reduction, the applied method also resembles the reactions of C_8K graphite intercalated compound with weak protic acids in tetrahydrofurane suspension[23,24] that give rise to the formation of partially reduced graphite with the composition of C_8H. The expected products of the dissolved metal reductions are covalently bonded CH derivatives and they are essentially different from the absorbed H_2 derivatives[25−28] used for hydrogen storage. The first steps of the proposed hydrogenation are the solution of lithium in ammonia and the formation of its carbanion complex:

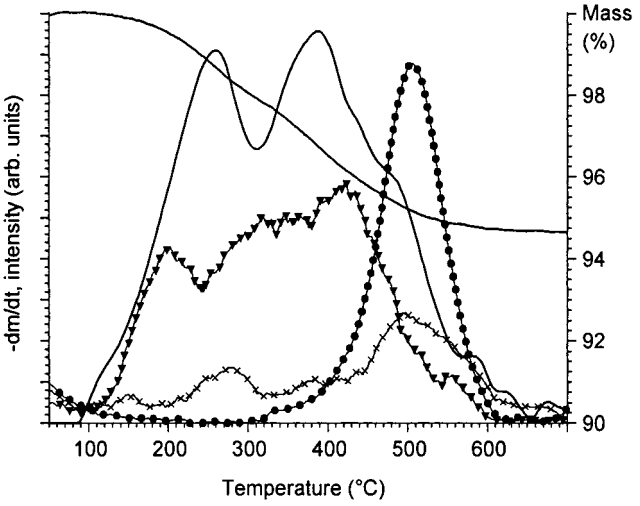

Figure 1. TG-MS plot of hydrogenated MWNT-s. —, TG and DTG; ●, hydrogen (*m*/*z* 2); ×, methane (*m*/*z* 16); ▼, methanol (*m*/*z* 31).

$$Li + nNH_3 \rightarrow Li^+ + e^-(NH_3)_n \quad (1)$$

$$e^-(NH_3)_n + C \rightarrow nNH_3 + C^- \quad (2)$$

In a subsequent step the carbanion decomposes by the reaction with methanol resulting in the formation of a covalent hydrogenated carbon derivative:

$$C^- + CH_3OH \rightarrow CH + CH_3O^- \quad (3)$$

A reaction competing with reaction 3 is the formation of hydrogen:

$$C^- + CH_3OH \rightarrow C + CH_3O^- + {}^1/_2H_2 \quad (4)$$

Additional hydrogen evolves due to the reaction of the excess ammoniated electron with methanol:

$$e^-(NH_3)_n + CH_3OH \rightarrow nNH_3 + CH_3O^- + {}^1/_2H_2 \quad (5)$$

The macroscopic appearance of hydrogenated nanotubes was very similar to that of the pristine samples, only the increased stability of the aqueous suspension, i.e., the significantly lower rate of sedimentation, indicated the modification of surface. Similarly, the appearance of graphite samples did not change significantly due to hydrogenation.

3.2. Structural Characterizations of the Hydrogenated Derivatives. To determine the chemical composition of the reacted carbonaceous materials, the samples were subjected to thermogravimetry-mass spectrometry (TG-MS) analysis. The pristine carbon nanotubes as well as graphite showed no measurable weight loss up to 900 °C. Figure 1 displays the TG-MS curves of hydrogenated MWNT-s. Besides the mass loss (TG) and its derivative (DTG) curves, the intensities of the three most significant volatile products are plotted. Hydrogen and methane are represented by their molecular ions (*m*/*z* 2 and *m*/*z* 16, respectively), while the major fragment ion (*m*/*z* 31) is plotted for methanol. The total mass loss (5.4%) takes place in a few steps in the temperature range of 100−650 °C as shown by the DTG curve. Each step is represented by the formation of different decomposition products. In the low temperature

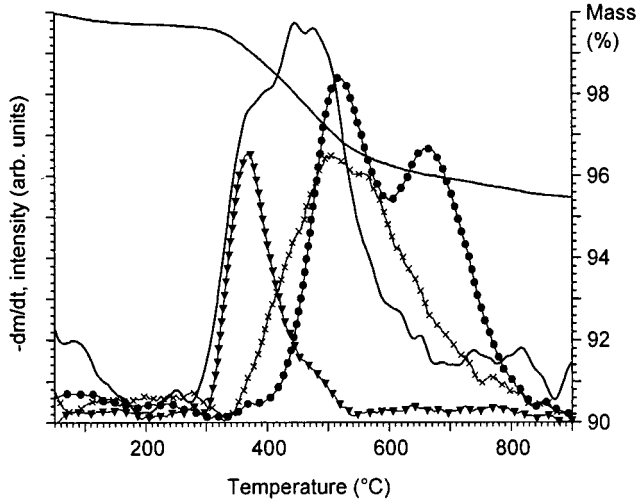

Figure 2. TG-MS plot of hydrogenated SWNT-s (heat-treated at 250 °C). —, TG and DTG; ●, hydrogen (*m*/*z* 2); ×, methane (*m*/*z* 16); ▼, methanol (*m*/*z* 31).

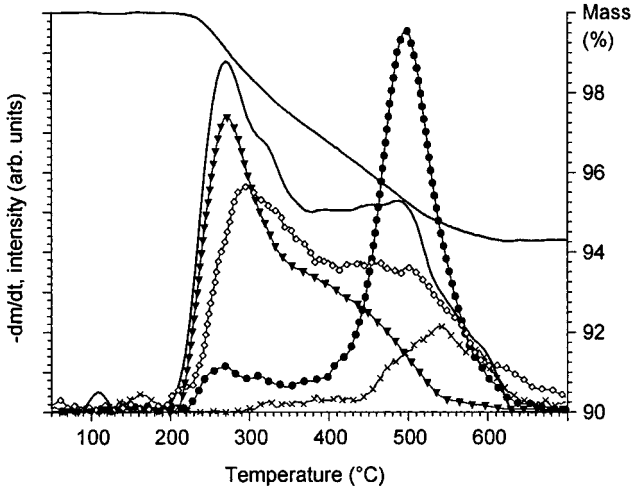

Figure 3. TG-MS plot of hydrogenated graphite (heat-treated at 200 °C). —, TG and DTG; ●, hydrogen (*m*/*z* 2); ×, methane (*m*/*z* 16); ◇, ammonia (*m*/*z* 17); ▼, methanol (*m*/*z* 31).

range up to 450 °C, the mass loss is predominantly due to the evolution of methanol that was the hydrogenating agent in reaction 3. The formation of hydrogen takes place in a separated temperature range of 400−600 °C with a maximum rate at 500 °C. Due to its low molecular mass, the contribution of hydrogen to the total mass loss is small though it has high molar ratio. The evolution of methane has a similar profile to the curve of hydrogen in the range of 400−600 °C indicating the same origin of the two products. The parallel formation of hydrogen and methane is characteristic of the thermal decomposition of various hydroaromatic compounds.[29] Low temperature heat treatments were performed in a dynamic vacuum to get rid of the weakly bound methanol. Due to these heat treatments, the predominant portion of methanol was removed. On the other hand, heat treatments above 350 °C resulted also in some loss of hydrogen, because of the overlap of the methanol and hydrogen curves.

The TG-MS curves of hydrogenated SWNT-s are shown in Figure 2. This sample was previously heat treated in a vacuum at 250 °C for 4 h. Due to the heat treatment, the onset of methanol evolution is very sharp at 300 °C and the total evolved amount is significantly decreased, corresponding to about 160 carbon/methanol ratio. The decomposition curve of hydrogen exhibits two peaks, one with a maximum at 500 °C similarly to that of the hydrogenated MWNT-s and the other at 680 °C. The evolution of methane is more or less parallel with the low temperature formation of hydrogen and shows no correlation with its high-temperature peak.

Figure 3 displays the thermoanalytical curves of hydrogenated graphite after a heat treatment in a vacuum at 200 °C for 4 h. Most of the characteristics of these curves are similar to those of the nanotube derivatives: methanol evolves in the low-temperature region resulting in a wide peak and there is a characteristic hydrogen peak at around 500 °C. However, in contrast to the nanotubes, a significant amount of ammonia is observed in this sample (*m*/*z* 17). Its evolution curve is similar to that of the methanol but it is shifted to higher temperatures overlapping with the full range of the hydrogen formation. A small amount of methane (*m*/*z* 16) is released at similar temperatures as hydrogen (400−600 °C). It should be noted that ammonia also produces *m*/*z* 16 fragment ion in the mass spectrometer; however, its contribution was subtracted from the intensity profile of *m*/*z* 16.

In contrast to the nanotubes and graphite, the hydrogenation of the extracted fullerene soot did not lead to a significant change in its composition. The thermoanalytical curves showed the evolution of much less hydrogen as compared to the other materials.

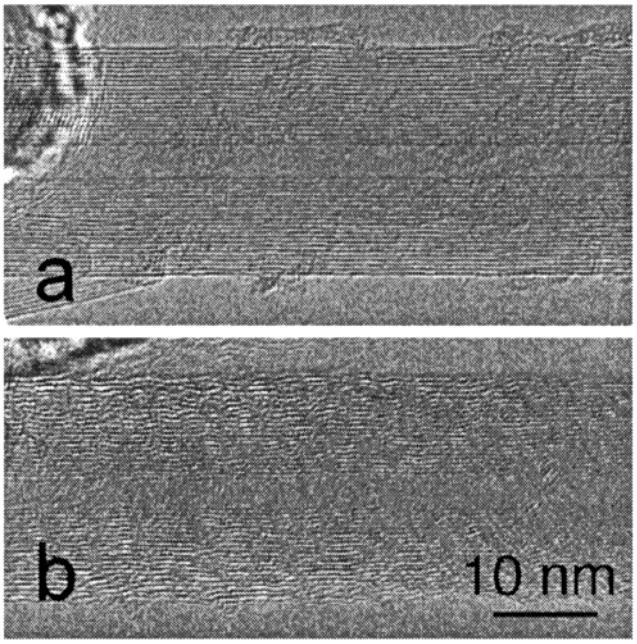

Figure 4. TEM images of individual pristine (a) and hydrogenated (b) multiwall nanotubes.

The influence of hydrogenation on the structure of nanotubes as well as graphite was studied by high-resolution transmission electron microscopy (TEM). Figure 4 shows the electron micrographs of MWNT samples before and after the hydrogenation. While the pristine sample consists of straight parallel walls, the hydrogenated one became corrugated and partly disordered. The corrugation extended through the whole sample; not even the inner walls remained intact. Considerable structural changes were observed in SWNT-s as well (Figure 5). Two bundles consisting of a few SWNT-s with more or less parallel walls are shown in Figure 5a. The straight walls became strongly disordered due to the influence of hydrogenation (Figure 5b). In some cases the surface of the tubes became amorphous giving rise to a poor contrast in the electron micrographs. Figure 6 shows the influence of hydrogenation on the structure of graphite. The parallel stacking of graphene planes became

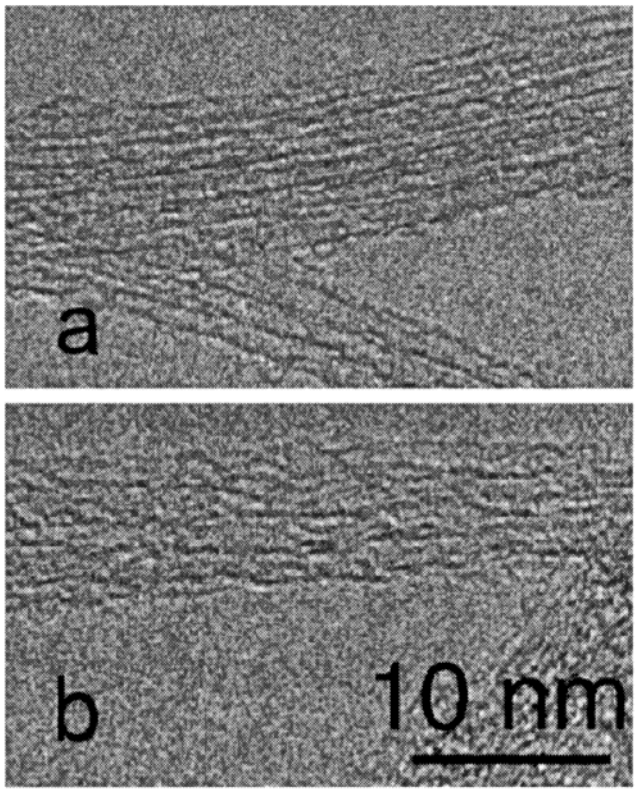

Figure 5. TEM images of pristine (a) and hydrogenated (b) bundles of single-wall nanotubes.

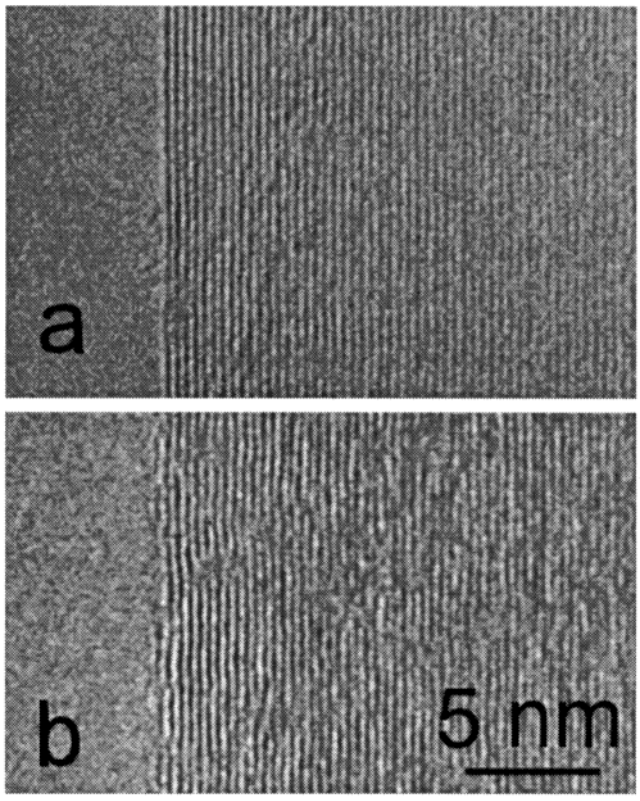

Figure 6. TEM images of pristine (a) and hydrogenated (b) graphite flakes.

corrugated due to hydrogenation similarly to the structural changes observed on the MWNT-s in Figure 4. Despite the obvious change in the structure of graphite, the ***c*** lattice parameter increased only by 1.0 ± 0.5%.

TABLE 1: TG-MS Data of Hydrogenated Carbonaceous Materials

sample	H_2 (mass %)[a]	CH_4 (mass %)[a]	H_2:CH_4	estimated C:H ratio
graphite powder	1.4	0.5	96:4	5.5:1
turbostratic graphite flakes	1.7	0.3	98:2	4.5:1
MWNT-s	0.72	0.18	97:3	10.8:1
SWNT-s	0.64	0.56	90:10	10.6:1
fullerene soot	<0.1	0.6	55:45	>35:1

[a] Mass % of the evolved gas relative to the total mass of the sample.

Preliminary ESR experiments performed on MWNT-s reveal that the spin susceptibility of the hydrogenated sample in respect to the pristine sample shows a much stronger Curie-tail at low temperatures. This corroborates with the notion obtained from the TEM images (Figure 4) that the chemical treatment introduces a disorder in the walls of MWNT-s, which localizes electrons/spins. The influence of this irregularity can be the origin of the much stronger temperature dependence of the d.c. resistivity: in the pristine sample it increases by a factor of 2−3 on cooling from 300 to 4.2 K, while in the hydrogenated one this factor is close to 12. It shows that the electron transfer between the tubes is more difficult because of the corrugation and/or due to the bonded hydrogens at the surface, which push further away the neighboring tubes.

4. Discussion

Both the thermoanalytical and the electron microscopic studies revealed that the applied hydrogenation method gave rise to the formation of strongly bound hydrogen derivatives in the nanotubes and graphite. The relatively narrow temperature range of the hydrogen evolution at around 500 °C (Figures 1−3) is characteristic of the thermal decomposition of compounds with well-defined structures. In contrast to this finding, both the volatile impurities of these samples and the adsorbed hydrogen in the materials prepared for storage[25−28] exhibit strongly different behavior: they evolve at lower temperature and in a much wider range. The observed temperature of dehydrogenation is lower than that of aliphatic and aromatic hydrocarbons,[30] but it can comply with the thermal stability of C−H bonds in hydroaromatic compounds.[29] In the vicinity of the covalent C−H bonds the conjugation of the π-electron system is destroyed due to the formation of sp^3 carbons in the sp^2 backbone. A tendency of rearomatization of the system can give rise to the weakening of C−H bonds and to the decreased decomposition temperature. Recent density functional (DF) calculations showed[31] that the binding energy of C−H bonds in fully hydrogenated SWNT-s is significantly lower than in methane, supporting the above explanation.

The chemical compositions of the materials prepared are summarized in Table 1. The yields of hydrogen and methane were determined from the mass losses and the integrated intensities of the corresponding mass spectrometric peaks as described in the Experimental Section. The estimated hydrogen content of the graphite samples corresponds to the average composition of C_5H, while the nanotubes contain approximately half of this amount of hydrogen. These compositions may be related to the different reactivities of planar and bent conjugated systems.[18] While both sides of the planar graphene sheets are equally reactive, the lower spatial extension of p orbitals and the unfavorable bond angles suppress the formation of covalent bonds in the concave surfaces of spherical and cylindrical π-electron systems. Thus, covalent bonds can only form in the convex surfaces of the nanotubes. Assuming that the density

of added hydrogen is the same in the reactive surfaces, the expected hydrogen content of nanotubes is half than that of graphite. In agreement with this idea, DF calculations showed[31] C−H bonds to be unstable in the concave surface of SWNT-s. On the other hand, the relatively high hydrogen contents obtained and their similar values for both kinds of nanotubes can only be explained by the hydrogenation of the inside layers of graphite and MWNT-s. The hydrogenation of the inside layers is also indicated by their corrugated shapes in the electron micrographs (Figures 4 and 6).

A further evidence of the covalent C−H bonds is the evolution of methane during the dehydrogenation. The parallel formation of methane and hydrogen shows their common origin (Figures 1−3). Similar formation of methane is observed during the pyrolysis of hydroaromatic compounds.[29] The molar ratio of the evolved H_2 and CH_4 depends on the structure of the hydrogenated materials and the mechanism of decomposition. As shown in Table 1, the molar ratio of the released H_2:CH_4 was 97:3 for graphite and MWNT-s while 90:10 for SWNT-s. In graphite and MWNT-s, the decomposition takes place predominantly in the inside sheets where the formation of methane is sterically restricted, explaining its smaller relative amount. The relatively high yield of methane from hydrogenated SWNT-s implies the rupture of the regular carbon skeleton in the temperature range of 400−600 °C. A secondary hydrogenation may occur at the dangling bonds formed and these aromatic and/or aliphatic C−H bonds decompose at higher temperature around 700 °C (Figure 2). This hydrogen peak resembles the charring reactions of aromatic and aliphatic hydrocarbons.[30]

The extracted fullerene soot, which consists of predominantly amorphous carbon, exhibits essentially different behavior with respect to hydrogenation than the nanotubes and graphite: Its total hydrogen content is much smaller (Table 1), the dehydrogenation takes place in a wide range of temperature without any characteristic peak, the amounts of H_2 and CH_4 released are almost equal. The differences indicate that the dissolved metal method applied is suitable for the hydrogenation of graphene-like conjugated systems and not for the hydrogenation of amorphous carbon.

Although hydrogen atoms cannot be observed directly in the TEM images, the corrugated and disordered structures of the hydrogenated materials (Figures 4−6) support the suggested formation of covalent C−H bonds. In the vicinity of C−H bonds, the C−C bonds become elongated due to the sp^3 character of the reacted C atoms. The elongation of the bonds can be higher than 0.1 Å. The longer bonds modify the smooth planar or cylindrical surfaces giving rise to disorder and/or corrugation.

During the hydrogenation of graphite, the reactions 1 and 2 take place under similar experimental conditions as the intercalation of graphite with alkali metals in liquid ammonia[32] suggesting the formation of Li−NH_3−C compounds. Furthermore, a possible formation of Li−H−C ternary compounds[33,34] cannot be excluded because the side reactions 4 and 5 produce hydrogen gas. However, the structure and the chemical stability of the obtained graphite derivative contradict with the formation of these ternary compounds. While the formation of both Li−NH_3−C and Li−H−C systems is accompanied with a considerable increase in the ***c*** lattice parameter of graphite,[32−35] we observed only a small increase (Figure 6). While the above intercalated compounds are unstable against air and moisture,[33,34] we purified the hydrogenated materials in aqueous hydrochloric acid and stored the samples in air without any detectable chemical change. On the other hand, the applied reduction method and the obtained C_5H stoichiometry are similar to those of the previously prepared C_8H compound[23,24] suggesting similar structures. The structure of C_8H is still ambiguous;[36] most probably partially reduced graphite is formed containing either covalent C−H bonds[23] or intercalated protons.[37] A novel hydrogen derivative of nanostructured graphite was prepared recently by mechanochemical method:[38] according to neutron diffraction measurements, half of the hydrogen content of the 1:1 stoichiometry compound is considered as covalently bound. The other possibility, proton intercalation may be consistent with the small increase in the distance between the graphene layers in C_5H. On the other hand, the similar chemical stability of the hydrogenated graphite and nanotube derivatives strongly indicates the same bonding nature of hydrogen in these compounds. In the nanotubes of high surface area, proton doping seems to be less stable than the formation of covalent C−H bonds. We assume that highly polarized covalent C−H bonds are formed in the hydrogenated graphite and nanotubes with some ionic character.

5. Conclusion

We have shown that both multiwall and single-wall nanotubes as well as graphite can be chemically hydrogenated via a dissolved metal reduction method in liquid ammonia. The strongly bound hydrogen releases from the materials at around 500 °C. The hydrogen contents, estimated from TG/MS correspond to a C_5H composition for graphite and $C_{11}H$ for nanotubes. The addition reaction of hydrogen introduces longer σ type C−C bonds as indicated by the significant disorder at the walls and layers of the hydrogenated nanotubes and graphite, determined by TEM. The σ bonds increase the resistivity and the anisotropy of the tubes. Further structural studies will be necessary to reveal the detailed bonding nature of hydrogen and the local configuration of the C−H bonds formed.

Acknowledgment. This work was supported by the Hungarian Research Fund OTKA T032613 and T025341, by the Swiss NSF, OFES, and by the NANOCOMP research grant of the European Community TMR program.

References and Notes

(1) Iijima, S. *Nature* **1991**, *354*, 56.
(2) Ebbensen, T. W.; Ajayan, P. M. *Nature* **1992**, *358*, 220.
(3) Bonard, J.-M.; Stora, T.; Salvetat, J.-P.; Maier, F.; Stöckli, T.; Duschl, C.; Forró, L.; de Heer, W. A. *Adv. Mater.* **1997**, *9*, 827.
(4) Rinzler, A. G.; Liu, J.; Dai, H.; Nikolaev, P.; Huffman, C. B.; Rodriguez-Macias, F. J.; Boul, P. J.; Lu, A. H.; Heymann, D.; Colbert, D. T.; Lee, R. S.; Fischer, J. E.; Rao, A. M.; Eklund, P. C.; Smally, R. E. *Appl. Phys. A* **1998**, *67*, 29.
(5) Dresselhaus, M. S.; Dresselhaus, G.; Eklund, P. C. *Science of Fullerenes and Carbon Nanotubes*; Academic Press: San Diego, 1995; Chapter 19.
(6) Ajayan, P. M.; Iijima, S. *Nature* **1993**, *361*, 333.
(7) Tsang, S. C.; Chen, Y. K.; Harris, P. J.; Green, M. L. H. *Nature* **1994**, *372*, 159.
(8) Ajayan, P. M.; Ebbesen, T. W.; Ichihshi, T.; Iijima, S.; Tanigaki, K.; Hiura, H. *Nature*, **1993**, *362*, 522.
(9) Seraphin, S.; Zhou, D.; Jiao, J.; Withers, J. C.; Loufty, R. *Nature* **1993**, *362*, 503.
(10) Guerret-Piecourt, C.; Le Bouar, Y.; Loiseau, A.; Pascard, H. *Nature* **1994**, *372*, 761.
(11) Lee, R. S.; Kim, H. J.; Fischer, J. E.; Thess, A.; Smally, R. E. *Nature* **1997**, *388*, 255.
(12) Rao, A. M.; Eklund, P. C.; Bandow, S.; Thess, A.; Smally, R. E. *Nature* **1997**, *388*, 257.
(13) Hamwi, A.; Alvergnat, H.; Bonnamy, S.; Beguin, F. *Carbon* **1997**, *35*, 723.
(14) Mawhinney, D. B.; Naumenko, V.; Kuznetsova, A.; Yates, J. T., Jr.; Liu, J.; Smally, R. E. *J. Am. Chem. Soc.* **2000**, *122*, 2383.
(15) Jin, Z.; Xu, G. Q.; Goh, S. H. *Carbon* **2000**, *38*, 1135.

(16) Pekker, S.; Salvetat, J.-P.; Jakab, E.; Bonard, J.-M.; Forró, L. In *CP486, Electronic Properties of Novel Materials*; Kuzmany, H., Fink, J., Mehring, M., Roth, S., Eds.; AIP: Melville, New York, 1999; pp 474.
(17) Holliday, A. K.; Hughes, G.; Walker, S. M. Carbon. In *Comprehensive Inorganic Chemistry*; Bailar, J. C., Emeléus, H. J., Nyholm, R., Trotman-Dickenson, A. F., Eds.; Pergamon Press: Oxford 1973; Vol. 1, Chapter 13.
(18) *Fullerenes and Related Structures, Topics in Current Chemistry*; Hirsch, A., Eds.; Springer: 1999; Vol. 199.
(19) Cornu, A.; Massot, R. *Compilation of Mass Spectral Data*; Heyden and Son Ltd.: London, 1966.
(20) Pinkerton, F. E.; Wicke, B. G.; Olk, C. H.; Tibbets, G. G.; Meisner, G. P.; Meyer, M. S.; Herbst, J. F. *J. Phys. Chem. B* **2000**, *104*, 9460.
(21) de Heer, W. A.; Châtelin, A.; Ugarte, D. *Science* **1995**, *270*, 1179.
(22) Haufler, R. E.; Conceicao, J.; Chibante, L. P. F.; Chai, Y.; Byrne, N. E.; Flanagan, S.; Haley, M. M.; O'Brien, S. C.; Pan, C.; Xiao, Z.; Ciufolini, W. E.; Hauge, R. N.; Margrave, J. L.; Wilson, L. J.; Curl, R. F.; Smally, R. E. *J. Phys. Chem.* **1990**, *94*, 8634.
(23) Bergbreiter, D. E.; Killough, J. M. *J. Chem. Soc. Chem. Commun.* **1976**, 913.
(24) Bergbreiter, D. E.; Killough, J. M. *J. Am. Chem. Soc.* **1978**, *100*, 2126.
(25) Dillon, A. C.; Jones, K. M.; Bekkedahl, T. A.; Kiang, C. H.; Bethune, D. S.; Heben, M. J. *Nature* **1997**, *386*, 377.
(26) Rzepka, M.; Lamp, P. *J. Phys. Chem. B* **1998**, *102*, 10894.
(27) Chen, P.; Wu, X.; Lin, J.; Tan, K. L. *Science* **1999**, *285*, 91.
(28) Yang, R. T. *Carbon* **2000**, *38*, 623.
(29) Bredael, P.; Vinh, T. H. *Fuel* **1979**, *58*, 211.
(30) Jakab, E.; Till, F.; Várhegyi, G. *Fuel Process. Technol.* **1991**, *28*, 221.
(31) Lee, S. M.; Lee, Y. H. *Appl. Phys. Lett.* **2000**, *76*, 2877.
(32) Rüdorff, W.; Schulze, E.; Rubisch, O. *Z. Anorg. Allg. Chem.* **1955**, *282*, 232.
(33) Terai, T.; Takahashi, Y. *Synth. Metals* **1983**, *7*, 49.
(34) Guérard, D.; Takoudjou, C.; Elalem, N. E.; Elansari, L. *Mater. Sci. Forum* **1992**, *91*−*93*, 85.
(35) Nakazawa, K.; Suzuki, K.; Enoki, T.; Sugihara, K.; Mizuno, S. *J. Phys. Soc. Jpn.* **1993**, *62*, 4386.
(36) Isaev, Yu. V.; Novikov, Yu. N. *Mater. Sci. Forum* **1992**, *91*−*93*, 209.
(37) Ebert, L. B.; Matty, L.; Mills, D. R.; Scanlon, J. C. *Mater. Res. Bull.* **1980**, *15*, 251.
(38) Orimo, S.; Majer, G.; Fukunaga, T.; Züttel, A.; Schlapbach, L.; Fujii, H. *Appl. Phys. Lett.* **1999**, *75*, 3093.